EurJIC European Journal of Inorganic Chemistry

ChemPubSoc Europe

FULL PAPER

DOI:10.1002/ejic.201300931

Lanthanide Borohydrido Complexes Supported by *ansa*-Bis(amidinato) Ligands with a Rigid *o*-Phenylene Linker: Effect of Ligand Tailoring on Catalytic Lactide Polymerization

Aleksei O. Tolpygin,[a] Grigorii G. Skvortsov,[a] Anton V. Cherkasov,[a] Georgy K. Fukin,[a] Tatyana A. Glukhova,[a] and Alexander A. Trifonov*[a]

Keywords: Lanthanides / Ligand design / Polymerization

A series of lanthanide monoborohydrido complexes $\{C_6H_4\text{-}1,2\text{-}[NC(R)NR']_2\}Ln(BH_4)(L)_n$ (Ln = Y, Nd, Sm; R = *t*Bu, Ph; R′ = 2,6-$Me_2C_6H_3$, $SiMe_3$; L = dme = dimethoxyethane, *n* = 1; L = thf, *n* = 2), in which lanthanides are coordinated by bulky *ansa*-bis(amidinato) ligand systems with a conformationally rigid *o*-phenylene linker ($\{C_6H_4\text{-}1,2\text{-}[NC(R)NR']_2\}^{2-}$), were synthesized by the salt metathesis reactions of equimolar amounts of $Ln(BH_4)_3(thf)_3$ and $\{C_6H_4\text{-}1,2\text{-}[NC(R)NR']_2\}X_2(thf)_n$ (X = Li, Na) in thf. X-ray diffraction studies revealed that the complexes are monomeric. Depending on the denticity of the donor ligand (L = dme or thf), the terminal borohydrido ligand coordinated to the metal ion can be located in either an equatorial (L = thf) or an apical (L = dme) position. All complexes are efficient catalysts for the ring-opening polymerization of *rac*-lactide, which allows to convert up to 1000 equiv. of monomer into a polymer at room temperature within 10–150 min and affords atactic polylactides with high molecular weights and moderate molecular-weight distributions (1.28–2.16). Yttrium–borohydrido complexes coordinated by the $\{C_6H_4\text{-}1,2\text{-}[NC(tBu)N(2,6\text{-}Me_2C_6H_3)]_2\}^{2-}$ ligand system showed enhanced catalytic activity compared to that of the analogue complexes containing the $\{C_6H_4\text{-}1,2\text{-}[NC(Ph)NSiMe_3]_2\}^{2-}$ ligand. The obtained borohydrido complexes catalyze the hydrophosphonylation of benzaldehyde at room temperature with good reaction rates.

Introduction

To control metal-mediated reactions it is important to "tailor" new ligand systems, which are suitable for the synthesis of isolable and structurally defined species, that is, prospective one-site catalysts. Their large ionic radii[1] make this issue especially significant for lanthanides, the stability and reactivity of which are known to be highly influenced by the coordinative and steric saturation of the metal center.[2] Lanthanide borohydrides[3] are efficient initiators for the ring-opening polymerization (ROP) of cyclic esters,[4] which allows for the synthesis of biodegradable and biocompatible thermoplastics.[3,5] In earlier studies, we have demonstrated that lanthanide–borohydrido complexes supported by guanidinato[6] ligands initiate the room temperature ROP of racemic lactide and β-butyrolactone, which provides atactic polymers with controlled molecular weights and relatively narrow polydispersities. Moreover, guanidinato ligands provide a good coordination environment, stabilizing lanthanide centers and facilitating immortal ring-opening polymerization (iROP) of lactide by the introduction of large amounts of isopropanol as a chain transfer agent.[6] At present, we aim at designing new ligand frameworks that provide a rigid geometry of the coordination sphere of the active metal center and thus allow to better control catalytic reactions. As monoanionic NCN ligands proved to be a suitable coordination platform,[7] we focused on *ansa*-bis(amidinato) ligand frameworks that contain conformationally rigid linkers. New bis(amidinato) ligand systems with 1,8-disubstituted naphthalene[8] and *o*-phenylene[9] linkers were prepared and successfully employed for the synthesis of lanthanide complexes. Herein, we report on the synthesis and characterization of new lanthanide borohydrides coordinated by *o*-phenylene linked bis(amidinato) ligands of different steric demand $\{C_6H_4\text{-}1,2\text{-}[NC(R)NR']_2\}^{2-}$ (R = *t*Bu, Ph; R′ = 2,6-$Me_2C_6H_3$, $SiMe_3$) and on their application in the catalysis of the polymerization of racemic lactide. When our study was in progress, a paper of Shen and co-workers on the synthesis of related lanthanide borohydrides supported by bis(amidinato) ligand systems with a flexible $(CH_2)_3$ linker, $\{CH_2[CH_2NC(Ph)NSiMe_3]_2\}Ln(BH_4)(dme)$ (dme = dimethoxyethane), and their cata-

[a] G. A. Razuvaev Institute of Organometallic Chemistry of Russian Academy of Sciences,
Tropinina 49, 603950 Nizhny Novgorod, GSP-445, Russia
E-mail: trif@iomc.ras.ru
http://www.iomc.ras.ru

Supporting information for this article is available on the WWW under http://dx.doi.org/10.1002/ejic.201300931.

lytic activity in the ring-opening polymerization of cyclic esters was published.[10] This essentially enriched the base for a comparative analysis of a structure–reactivity relationship.

Results and Discussion

Two efficient synthetic approaches to mixed-ligand lanthanide borohydrides are generally applied. The first pathway consists in the reactions of the corresponding halido (Hal) derivatives L_nLnHal_{3-n} with XBH_4 (X = Li, Na, K) in donor solvents.[11] However, this synthetic method is often hampered by side reactions, for example, ligand redistribution.[3k] Another convenient procedure for the synthesis of both bis(borohydrido) and mono(borohydrido) complexes is based on the reactions of lanthanide tris(borohydrides) $Ln(BH_4)_3(thf)_3$[12] with alkali-metal salts LX (X = Li, Na, K) of the corresponding ligands.[3a,6,10,13] For the preparation of lanthanide–borohydrido species coordinated by *ansa*-bis(amidinato) ligand systems, the second synthetic pathway was employed. In this work, two *o*-phenylene linked bis(amidinato) ligand systems of different steric demand, $\{C_6H_4\text{-}1,2\text{-}[NC(t\text{Bu})N(2,6\text{-}Me_2C_6H_3)]_2\}^{2-}$ [9a] and $\{C_6H_4\text{-}1,2\text{-}[NC(Ph)NSiMe_3]_2\}^{2-}$ [9b], were used.

Bis(amidine) **1** can be easily deprotonated by a treatment with two equivalents of $NaN(SiMe_3)_2$ in thf at 20 °C.[9a] The disodium derivative of **1** was used in situ for reactions with $Ln(BH_4)_3(thf)_3$ (Ln = Y, Nd, Sm; 1:1 molar ratio) in thf at ambient temperature (Scheme 1). The evaporation of thf, the extraction of the solid residue with toluene, and the subsequent recrystallization of the reaction product from dme/hexane mixtures allowed for isolation of the bis(amidinato)–borohydrido–lanthanide complexes **2**–**4** in 52, 43, and 39% yield, respectively. Complexes **2**–**4** were obtained as air- and moisture-sensitive, pale-yellow, crystalline solids, which are well soluble in thf and toluene but poorly soluble in hexane.

The related bis(benzamidinato) ligand system $\{C_6H_4\text{-}1,2\text{-}[NC(Ph)NSiMe_3]_2\}^{2-}$ was prepared according to the previously published procedure based on the insertion of PhCN into lithium silylarylamide.[9b] Lithium benzamidinate **5** was treated with an equimolar amount of $Y(BH_4)_3(thf)_3$ in thf at 65 °C (Scheme 2). The extraction of the reaction product with toluene and a subsequent recrystallization from a thf/hexane mixture afforded complex **6** as yellow crystals in 67% yield. It should be mentioned that unlike other ligands,[3i,6] the employment of $\{C_6H_4\text{-}1,2\text{-}[NC(Ph)NSiMe_3]_2\}Li_2(thf)_n$ allowed for the synthesis and isolation of a salt-free borohydrido complex. Treatment of **6** with dme leads to the substitution of thf by dme in the metal coordination sphere and to the formation of the dme adduct **7**.

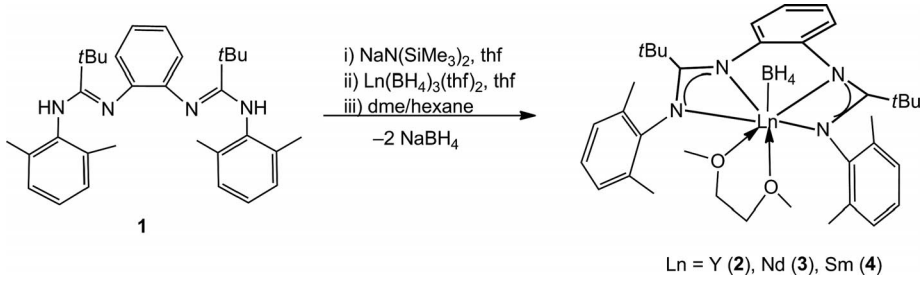

Scheme 1. Synthesis of complexes **2**–**4**.

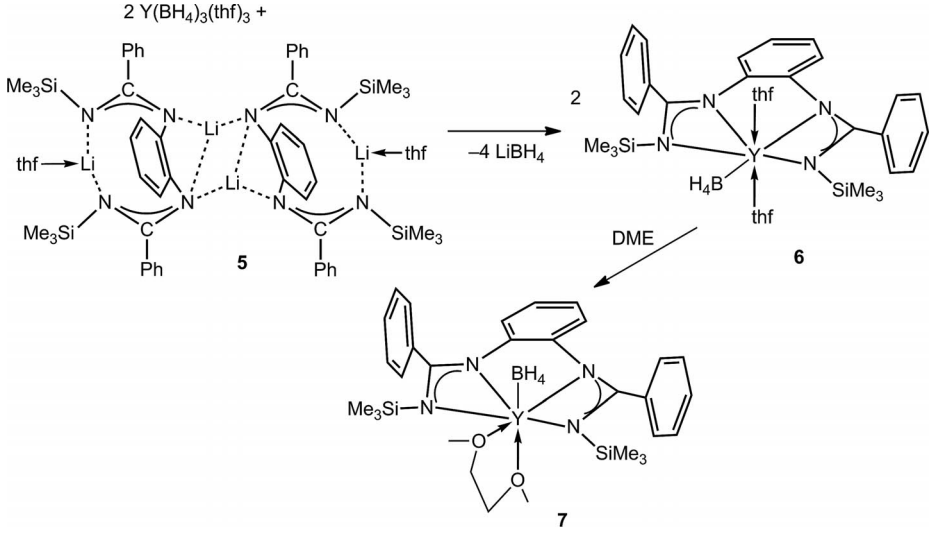

Scheme 2. Synthesis of complexes **6** and **7**.

The IR spectra of complexes **2**–**4**, **6**, and **7** show strong absorptions in the region 2150–2500 cm^{-1}, which are diagnostic of η^3-coordinated bridging and terminal borohydrido ligands.[14] In the ^1H NMR spectra of the diamagnetic yttrium complexes **2**, **6**, and **7**, the borohydrido ligands give broad singlets at δ = 1.17, 1.72, and 1.48 ppm, respectively.

Transparent crystals of complexes **2**–**4** suitable for X-ray diffraction analyses were obtained by slow condensation of hexane into dme solutions of the complexes at ambient temperature. Complex **2** crystallizes in the triclinic space group $P\bar{1}$, whereas **3** and **4** crystallize in the monoclinic space group $P2(1)$. The molecular structures of complexes **2**–**4** were determined by X-ray diffraction studies, which revealed that they have similar structures. Moreover, **3** and **4** are isostructural. The structure of complex **2** is depicted in Figure 1 (for the structures of complexes **3** and **4** see Figures S16 and S17). The crystallographic and structure-refinement data are given in Table 3. Selected bond lengths and angles are given in Table 1.

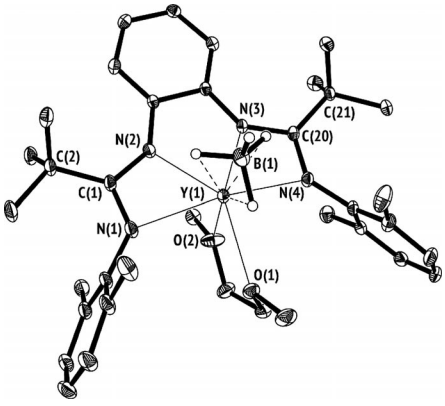

Figure 1. ORTEP diagram (thermal ellipsoids drawn at the 30% probability level) of **2**, showing the atom numbering scheme. Hydrogen atoms of the amidinato ligand and the dme molecule are omitted for clarity.

In complexes **2**–**4**, the metal atoms are coordinated by four nitrogen atoms of two chelating ligands, one η^3-coordinated terminal borohydrido anion, and two oxygen atoms of a dme molecule. The nitrogen atoms and one oxygen atom are in the equatorial plane [the maximum deviation of the atoms from the plane is 0.07(2) Å in **2**, 0.14(2) Å in **3**, and 0.15(2) Å in **4**], whereas the borohydrido group and the second oxygen atom occupy the apical positions. The B–Ln–O bond angles in complexes **2**–**4** are 171.17(6), 172.4(1), and 171.55(7)°, respectively. The dihedral angles between the two N–Ln–N planes in complexes **2**–**4** have values of 159.8(2), 162.6(2), and 163.7(2)°, respectively. The Ln–N–C–N fragments in complexes **2**–**4** are close to planar. Nevertheless, the values of dihedral angles between the N–Ln–N and N–C–N planes [168.1 and 167.6° for **2**; 144.8 and 177.4° for **3**; 145.9(2) and 177.1(2)° for **4**] indicate noticeable differences between the geometry of **2** and that of **3** and **4**. The average Y–N bond length in **2** [2.362(1) Å] is similar to the values found for the related seven-coordinate chlorido–yttrium complexes with *ansa*-bis(amidinato) ligands [2.394(4) Å[9a] and 2.392(5) Å[10]]. The Ln–N bonds

Table 1. Selected bond lengths and angles in complexes **2**–**4**, **6**, and **7**.

Complex	**2**	**3**	**4**	**6**	**7**
Ln–N [Å]	2.436(1)	2.521(2)	2.498(2)	2.534(3)	2.525(1)
	2.293(1)	2.368(2)	2.347(2)	2.330(3)	2.312(1)
	2.294(1)	2.400(2)	2.371(2)	2.329(3)	2.302(1)
	2.423(1)	2.478(2)	2.450(1)	2.533(3)	2.532(1)
C–N [Å]	1.319(2)	1.329(2)	1.335(3)	1.321(4)	1.320(2)
	1.360(2)	1.347(2)	1.343(3)	1.335(4)	1.336(2)
	1.360(2)	1.358(3)	1.351(3)	1.337(4)	2.331(2)
	1.329(2)	1.329(3)	1.334(3)	1.315(4)	2.325(2)
N–C–N [°]	109.9(1)	109.6(2)	109.9(2)	113.9(3)	115.0(1)
	109.8(1)	110.0(2)	109.6(2)	113.8(3)	114.2(1)
Ln–B [Å]	2.559(2)	2.678(3)	2.647(3)	2.646(4)	2.531(2)
Ln–H [Å]	2.32(2)	2.50(2)	2.47(3)	2.48(5)	2.27(2)
	2.29(2)	2.52(2)	2.50(3)	2.34(5)	2.29(2)
	2.41(2)	2.44(2)	2.42(4)	2.51(7)	2.27(2)
B–H [Å]	1.14(2)	1.11(2)	1.12(2)	1.11(5)	1.07(2)
	1.17(2)	1.14(2)	1.16(2)	1.18(6)	1.07(2)
	1.09(2)	1.16(2)	1.15(2)	1.20(8)	1.07(2)
	1.10(2)	1.17(2)	1.16(2)	1.11(5)	1.04(2)
Ln–O [Å]	2.457(2)	2.596(2)	2.560(2)	2.335(2)	2.436(1)
	2.398(2)	2.530(2)	2.500(1)	2.350(2)	2.428(1)

in complexes **2**–**4** are noticeably different. The two amidinato 1,2-C_6H_4N nitrogen atoms are situated much closer to the metal center [2.293(1) and 2.294(1) Å for **2**; 2.369(3) and 2.399(3) Å for **3**; 2.348(2), 2.371(2) Å for **4**], than the two nitrogen atoms of the 2,6-$Me_2C_6H_3N$ groups [2.436(1) and 2.424(1) Å for **2**; 2.521(4) and 2.475(2) Å for **3**; 2.498(2) and 2.448(1) Å for **4**]. Similar bonding situations are realized in the related lanthanide–*ansa*-bis(amidinato) complexes with a flexible $(CH_2)_3$ linker $\{CH_2[CH_2NC(Ph)NSiMe_3]_2\}Ln(BH_4)(dme)$.[10] The average Ln–N bond lengths in complexes **2**, **3**, and **4** [2.362(1), 2.442(2), and 2.417(2) Å, respectively] are slightly shorter than the values found in compounds $\{CH_2[CH_2NC(Ph)NSiMe_3]_2\}Ln(BH_4)(dme)$[10] [2.392(5) Å for Y, 2.470(8) Å for Nd, and 2.444(5) Å for Sm].[10] At the same time, for the Ln–B distances, an inverse tendency was detected: in complexes **2**–**4** [2.559(2), 2.682(4), and 2.651(3) Å, respectively], these bonds are slightly longer than in the related complexes $\{CH_2[CH_2NC(Ph)NSiMe_3]_2\}Ln(BH_4)(dme)$ [2.503(8) Å for Y, 2.636(11) Å for Nd, and 2.630(4) Å for Sm].[10] The lengths of the amidinato N–C bonds in complexes **2**–**4** have similar values, which indicates the negative charge delocalization within the N–C–N fragments.

Transparent crystals of complex **6** suitable for an X-ray diffraction study were obtained by slow condensation of hexane into a thf solution of the complex at ambient temperature. Complex **6** crystallizes in the space group $P2(1)2(1)2(1)$. The molecular structure of complex **6** was established by an X-ray diffraction study. The structure of complex **6** is depicted in Figure 2. The crystallographic and structure-refinement data are given in Table 3. Selected

bond lengths and angles are given in Table 1. Similarly to complexes **2**–**4**, the metal atom in **6** is coordinated by four nitrogen atoms of two amidinato ligands, one η^3-coordinated terminal borohydrido anion, and two oxygen atoms of two thf molecules. However, unlike in complexes **2**–**4**, the borohydrido group in **6** is in the equatorial plane [the maximum deviation of atoms from the plane is 0.10(2) Å] together with four nitrogen atoms, whereas the oxygen atoms occupy the apical positions. The distances from Y to "internal" nitrogen atoms are significantly shorter [2.329(3) and 2.330(3) Å] than those to "external" nitrogen atoms [2.533(3) and 2.534(3) Å]. The average Y–N bond in **6** [2.432(3) Å] is noticeably longer than that of **2** [2.362(1) Å] and that of $\{CH_2[CH_2NC(Ph)NSiMe_3]_2\}Y(BH_4)(dme)$ [2.392(5) Å].[10] The Y–B distance in **6** [2.644(5) Å] is also longer than the corresponding bonds in **2** [2.559(2) Å] and $\{CH_2[CH_2NC(Ph)NSiMe_3]_2\}Y(BH_4)(dme)$ [2.503(8) Å].[10] It is noteworthy that the coordination of the ligand systems $\{C_6H_4\text{-}1,2\text{-}[NC(t\text{Bu})N(2,6\text{-}Me_2C_6H_3)]_2\}^{2-}$ and $\{C_6H_4\text{-}1,2\text{-}[NC(Ph)NSiMe_3]_2\}^{2-}$ to yttrium results in a different mutual disposition of the amidinato fragments in complexes **2** and **6**. Thus, in **6** the dihedral angle between the N–Ln–N fragments [172.8(2)°] is much larger than that in **2** [159.8(2)°].

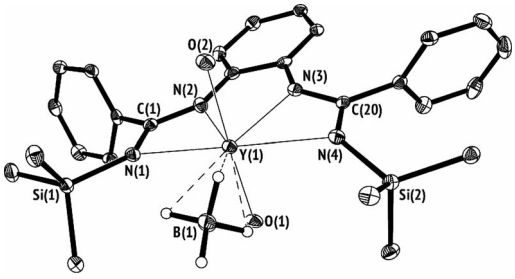

Figure 2. ORTEP diagram (thermal ellipsoids drawn at the 30% probability level) of **6**, showing the atom numbering scheme. Hydrogen atoms of the amidinato ligand and CH_2 groups of thf molecules are omitted for clarity.

Transparent crystals of complex **7** suitable for an X-ray diffraction study were obtained by the slow cooling of its toluene solution to –20 °C. Complex **7** crystallizes as a solvate, **7**·C_7H_8. The X-ray structure determination revealed that the ligand arrangement in complex **7** is similar to those in **2**–**4** (Figure 3). Despite the same coordination number of the yttrium atoms in **6** and **7**, the replacement of two thf molecules by one chelating dme molecule results in a dramatic structure change consisting of a migration of a borohydrido ligand from an equatorial position in **6** to an apical one in **7**. The dihedral angle between the N–Ln–N fragments in **7** [163.1(2)°] is larger than that in **2** [159.8(2)°] but smaller than that in **6** [172. 8(2)°]. Similarly to **2**–**4** and **6**, the distances from the metal center to "internal" nitrogen atoms in **7** are significantly shorter than those to "external" nitrogen atoms [compare: Y(1)–N(2) 2.301(1) and Y(1)–N(1) 2.312(1), to Y(1)–N(3) 2.527(1) and Y(1)–N(4) 2.533(1) Å]. The average Y–N bond length in **7** [2.418(1) Å] is somewhat shorter than that in **6** [2.432(3) Å]. The Y–B distance in **7** [2.531(2) Å] is noticeably shorter than the corresponding distance in **6** [2.646(4) Å] and comparable to that in **2** [2.559(2) Å] and $\{CH_2[CH_2NC(Ph)NSiMe_3]_2\}Y(BH_4)(dme)$ [2.503(8) Å].[10]

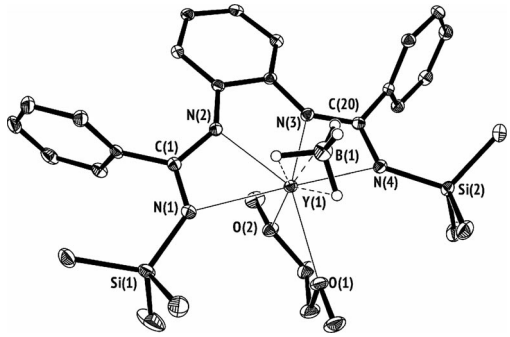

Figure 3. ORTEP diagram (thermal ellipsoids drawn at the 30% probability level) of **7**, showing the atom numbering scheme. Hydrogen atoms of the amidinato ligand and the dme molecule are omitted for clarity.

It is worthy to note that the positional change of the borohydrido group in the coordination sphere of yttrium is reflected in the IR spectra of complexes **6** and **7**. Thus, in the IR spectrum of **6**, the borohydrido ligand shows a set of four strong well resolved absorptions (2401, 2338, 2280, 2228 cm^{-1}), whereas in that of **7**, three badly resolved strong absorptions are observed (2447, 2216, 2168 cm^{-1}).

rac-Lactide Polymerization Initiated by Complexes 2–4, 6, and 7

The prepared complexes **2**–**4**, **6**, and **7**, having a potentially initiating BH_4 group, have been evaluated in the ROP of *rac*-lactide (LA) (Scheme 3). Representative results are summarized in Table 2. All complexes proved to be efficient catalysts under mild conditions, allowing for the total conversion of 100–1000 equiv. of lactide (toluene, 20 °C, [LA] = 1.0 mol/L) in 30–150 min and affording atactic PLAs (polylactides), as determined by NMR analyses. However, catalytic tests revealed that the activities of the complexes are affected by the nature of the metal center. Thus, in the case of **3**, a total conversion of 100 equiv. of monomer was achieved within 30 min, whereas within the same time, **4** and **2** only achieved conversions of 86 and 65%, respectively. The observed decrease of polymerization activity in the order Nd > Sm > Y correlates with the ionic radii of the lanthanide centers (1.11, 1.02, and 0.96 Å, respectively).[15] For PLA obtained with complex **2**, showed the lowest polymerization rate, a slightly larger polydispersity was measured (1.59 for **2**; 1.37 for **3**; 1.44 for **4**). An increase of the ratio $[M]_0/[I]_0$ to 1000 results in an increase of the reaction time necessary for full conversion to 150 min for **2**, 90 min for **3**, and 90 min for **4**. At $[M]_0/[I]_0$ = 1000, the conversion after 60 min reached 25% for **2**, 63% for **3**, and 54% for **4**. The polymerizations mediated by the complexes **2** and **7** proceeded much faster in an apolar, noncoordinating solvent such as toluene than in thf (Table 2, entries 5, 8 and 26, 28). Because of its high affinity for oxophilic metals such as lanthanides, we assume that thf com-

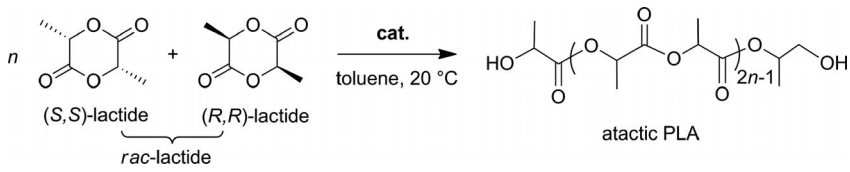

Scheme 3. Catalytic ring-opening polymerization of *rac*-lactide.

Table 2. Polymerization of *rac*-lactide with complexes **2**–**4**, **6**, and **7**.[a]

Entry	Complex	$[M]_0/[I]_0$	t [min][b]	Conversion [%][c]	$M_{nexp} \times 10^{-3}$[d]	$M_{ncalc} \times 10^{-3}$[e]	M_w/M_n	P_r
1	**2**	100	10	17	10.92	2.44	1.48	0.54
2	**2**	100	30	65	14.66	9.36	1.49	0.55
3	**2**	100	60	96	8.76	13.82	1.59	0.55
4	**2**	250	60	96	48.18	34.56	1.46	0.55
5	**2**	500	60	95	69.62	72.00	1.68	0.53
6	**2**	1000	60	25	37.27	36.00	1.49	0.55
7	**2**	1000	150	92	65.41	132.48	1.65	0.56
8	**2**[f]	500	60	43	9.60	28.80	1.59	0.63
9	**2**[f]	250	60	65	7.61	23.40	1.86	0.63
10	**3**	100	10	34	8.69	4.89	1.52	0.56
11	**3**	100	30	100	19.79	12.96	1.89	0.55
12	**3**	120	60	100	20.54	17.28	1.37	0.56
13	**3**	250	30	100	56.05	36.00	1.50	0.53
14	**3**	500	60	100	70.90	72.00	1.47	0.56
15	**3**	1000	60	63	59.47	90.72	1.60	0.54
16	**3**	1000	90	98	100.77	141.12	1.93	0.52
17	**4**	100	10	20	13.11	2.88	1.28	0.52
18	**4**	100	30	96	34.00	13.82	1.38	0.50
19	**4**	250	30	94	46.93	33.84	1.42	0.50
20	**4**	500	60	85	67.24	61.20	1.42	0.56
21	**4**	1000	60	54	49.09	77.76	1.44	0.54
22	**4**	1000	90	96	88.01	138.24	2.16	0.55
23	**6**	100	60	72	14.28	10.37	1.79	0.55
24	**6**	200	60	40	0.962	7.20	1.63	0.59
25	**6**	500	60	25	11.95	28.80	1.45	0.55
26	**7**	200	60	94	14.51	27.07	1.70	0.55
27	**7**	500	60	71	37.33	51.12	1.65	0.55
28	**7**[f]	200	60	82	12.85	23.62	1.70	0.62

[a] General conditions: toluene, [LA] = 1.0 mol/L, T = 20 °C. [b] Reaction time was not necessarily optimized. [c] Conversion of monomer M, as determined by ^{1}H NMR spectroscopy. [d] Experimental (corrected; see Experimental Section) M_n and M_w/M_n values determined by GPC in thf vs. polystyrene standards. [e] M_n value calculated by assuming one polymer chain per metal center with the relationship: 144 × conversion × [M]/[Ln]. [f] Catalytic tests carried out in thf.

petes with the lactide monomer in coordination to the metal center, which would account for the longer times needed for completion of the ROP. A similar detrimental effect of thf on the rate of ROP reactions promoted by group-3 metal complexes is often observed.[16] The ^{1}H NMR spectra in $CDCl_3$ of relatively low-molecular-weight samples of PLA (e.g., entry 25 of Table 2) display besides the main polymer-chain signals [a multiplet at δ = 1.56 ppm corresponding to –C(O)CH(*Me*)O and a multiplet at δ = 5.16 ppm corresponding to –C(O)C*H*(CH_3)O] a quartet characteristic for the terminal C*H*(Me)OH group at δ = 4.35 ppm (Figure S15). The latter group is formed after hydrolysis of the metal–alkoxido bond, an observation that is indicative of a classical coordination–insertion mechanism with an initial ring opening through acyl–oxygen bond cleavage.[17] The signals at δ = 3.74 ppm and δ = 2.71 ppm correspond to the second chain-end group –C*H*(Me)CH_2OH. It has been recently reported that in the ROP of lactide initiated by lanthanide–borohydrido complexes $Ln(BH_4)_3(thf)_3$ the borohydrido group acts as both an initiating group and as a reducing agent, yielding α,ω-dihydroxy telechelic PLAs.[18] Moreover, additional resonances at δ = 5.50 ppm and at δ = 4.18 and 4.45 ppm, which could correspond to CH_2OH end groups, are present in the spectra. However, their lower-than-expected intensity and diversity point to incomplete or multiple processes.

A comparison of the results of the catalytic performance of complexes **2** and **7** indicates enhanced activity of yttrium–borohydrido complexes coordinated by the $\{C_6H_4$-1,2-$[NC(t$Bu)N(2,6-$Me_2C_6H_3)]_2\}^{2-}$ ligand system compared to the complex containing $\{C_6H_4$-1,2-$[NC(Ph)NSiMe_3]_2\}^{2-}$ (entries 5 and 28, Table 2). Thus, in the presence of complex **2**, at $[M]_0/[I]_0$ ratio of 500, monomer was converted into polymer completely within 60 min, whereas for complex **7**, after the same interval of time, the conversion was noticeably lower: 71 %. The PLAs obtained with complexes **2** and **7** had similar polydispersities (compare: 1.68 for **2**; 1.65 for **7**).

Lactide polymerization reactions initiated by yttrium complexes coordinated by the same ligand system turned out to be strongly influenced by the nature of the Lewis base coordinated to the metal center. Thus, the activity of complex **7**, which contains a dme molecule, is significantly higher than that of the thf adduct **6**. In the polymerization initiated by **7** at ratio $[M]_0/[I]_0 = 200$, the conversion reaches 94% within 60 min, whereas **6** afforded only 40% conversion in the same time interval. At a ratio $[M]_0/[I]_0 = 500$, **7** converted 71% of the monomer into polymer within 60 min, and in the case of **6**, the yield of polylactide was 25%. Taking into account the stronger binding of chelating ligands to a metal center (compared to that of monodentate ones), it would be reasonable to expect an inverse trend of activities for complexes **6** and **7**. Probably, this difference of catalytic performance between **6** and **7** is related to their structural peculiarities.

When our studies were in progress, a report of Shen and co-workers on the synthesis and catalytic behavior in lactide polymerization of related borohydrido complexes supported by an *ansa*-bis(amidinato) ligand system with a nonrigid $(CH_2)_3$ linker $\{CH_2[CH_2NC(Ph)NSiMe_3]_2\}Ln(BH_4)(dme)$ (Ln = Y, Nd, Sm, Yb) was published.[10] A comparison of the results of catalytic tests obtained with complexes $\{CH_2[CH_2NC(Ph)NSiMe_3]_2\}Y(BH_4)(dme)$ and **7**, which have similar structures but different linkers between the amidinato ligands, would allow for a deeper insight into the effect of the linker on the catalytic activity and the control of metal-promoted reactions. Complex $\{CH_2[CH_2NC(Ph)NSiMe_3]_2\}Y(BH_4)(dme)$ demonstrated higher activity compared to that of **7**. At a ratio $[M]_0/[I]_0 = 1000$, the *rac*-lactide polymerization promoted by $\{CH_2[CH_2NC(Ph)NSiMe_3]_2\}Y(BH_4)(dme)$ (toluene, 20 °C) reached 86% conversion within 8 min, whereas in the case of an initiation with **7**, at a ratio $[M]_0/[I]_0 = 500$, the conversion was 95% after 60 min. Unlike $\{CH_2[CH_2NC(Ph)NSiMe_3]_2\}Y(BH_4)(dme)$, which showed similar activities in both thf and toluene, the activity of **7** ($[M]_0/[I]_0 = 500$, 60 min) in thf dropped to 43% compared to 95% in toluene.

Experiments aimed at investigating the degree of control of the polymerizations were carried out. The PLAs produced with complexes **2**–**4**, **6**, and **7** showed monomodal GPC traces with molecular-weight distributions in the range $M_w/M_n = 1.28$–2.17. For all initiators, the number-average molecular mass (M_n) values increase monotonously, though not linearly, with the monomer-to-metal ratio (see Figures 4, 5, and 6).

Relatively narrow molecular-weight distributions ($M_w/M_n = 1.37$–1.50) were observed for polymerizations carried out with monomer-to-metal ratios in the range 100–500. However, when higher monomer loadings (1000 equiv.) were used for complexes **2**–**4**, a slight increase of the PDI (polydispersity index) was observed (1.65–2.16). A matching of corrected experimental number-average molecular mass (M_n) values of PLAs with calculated values was observed in a few cases (entries 6, 14, 20).

Interestingly, for complexes **2**–**4**, at low $[M]_0/[I]_0$ ratios (100–250) and low conversions, the experimental M_n

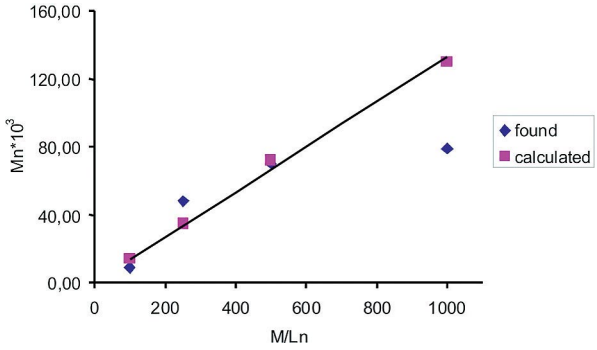

Figure 4. M_n vs $[M]_0/[I]_0$ for ROP initiated by **2**. Conditions: toluene, 20 °C, $[M]_0 = 1.0$ mol/L.

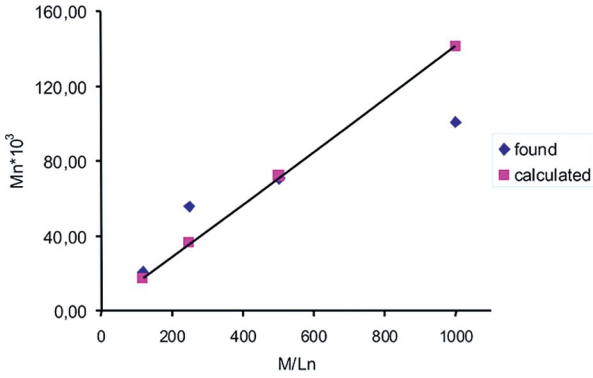

Figure 5. M_n vs $[M]_0/[I]_0$ for ROP initiated by **3**. Conditions: toluene, 20 °C, $[M]_0 = 1.0$ mol/L.

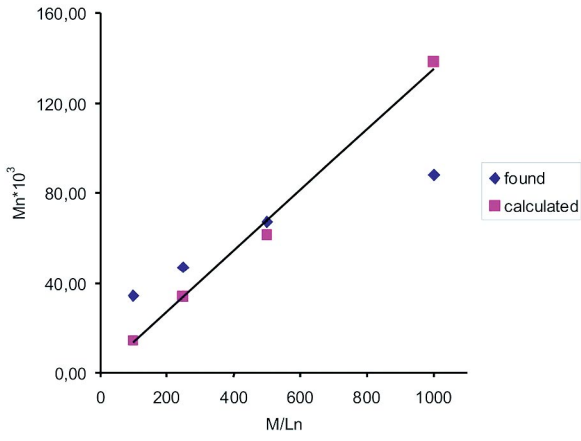

Figure 6. M_n vs $[M]_0/[I]_0$ for ROP initiated by **4**. Conditions: toluene, 20 °C, $[M]_0 = 1.0$ mol/L.

(M_{nexp}) values noticeably exceed the calculated ones (M_{ncalc}) (entries 1, 10, 17), which is probably due to a slow initiation stage. At $[M]_0/[I]_0 = 500$, all initiators showed a good agreement of M_{nexp} and M_{ncalc} (entries 5, 14, 20). At $[M]_0/[I]_0 = 1000$, M_{nexp} became significantly lower than M_{ncalc}, which indicates that a transesterification reaction occurs. Shen and co-workers reported that the complexes $\{CH_2[CH_2NC(Ph)NSiMe_3]_2\}Ln(BH_4)(dme)$ allow to perform the polymerization of *rac*-lactide in a living fashion.[10] The results obtained in the catalytic tests indicate that com-

plexes **2**–**4**, **6**, and **7**, coordinated by bis(amidinato) ligand systems with a rigid linker, surprisingly provide a lower degree of control compared to the derivatives of the ligand with a nonrigid bridge. The authors of the paper[10] reported that the solvent plays a crucial role for the stereoselectivity of the *rac*-lactide polymerization initiated by complexes $\{CH_2[CH_2NC(Ph)NSiMe_3]_2\}Ln(BH_4)(dme)$.

Thus, the reactions in toluene afforded atactic PLAs, whereas in thf under the similar conditions heterotactic-enriched polymers with P_r values up to 85% were obtained. In contrast, for complexes **2** and **7**, only a slight enhancement of P_r (up to 63 and 62%, respectively) was detected when the polymerizations were run in thf.

Hydrophosphonylation of Benzaldehyde Catalyzed by Complexes 2–4, 6 and 7

The catalytic hydrophosphonylation of aldehydes and imines (Abramov and Pudovik reactions)[19] is a straightforward and atom-economic method for the formation of P–C bonds, which allows for the synthesis of α-amino and α-hydroxy phosphonic acids possessing important biological activities. Various types of lanthanide compounds have demonstrated high potential in the catalysis of these reactions,[20] but to the best of our knowledge, no reports on the activity of borohydrido complexes have been published so far. The borohydrido complexes **2**–**4**, **6**, and **7** were tested as catalysts for the hydrophosphonylation of benzaldehyde. The reactions of equimolar amounts of benzaldehyde and diethyl phosphite (Scheme 4) were carried out in toluene at 20 °C in the presence of 1 mol-% of catalyst.

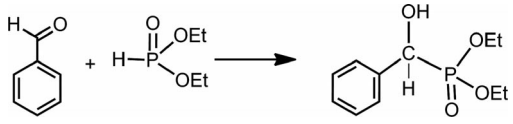

Scheme 4. Hydrophosphonylation of benzaldehyde catalyzed by complexes **2**–**4**, **6**, and **7**.

The borohydrido complexes **2**–**4**, **6**, and **7** catalyze the addition of diethyl phosphite to benzaldehyde under very mild conditions. In the series of complexes **2**–**4**, a correlation of catalytic activity and ionic radius was observed. Thus, in the presence of yttrium compound **2**, 44% conversion was achieved within 24 h, whereas the complexes of neodymium and samarium achieved quantitative yields of diethyl hydroxy(phenyl)methylphosphonate within the same period of time. Among the yttrium complexes, **2**, **6**, and **7**, complexes coordinated by the ligand $\{C_6H_4\text{-}1,2\text{-}[NC(Ph)NSiMe_3]_2\}^{2-}$ showed a higher catalytic activity compared to those with the ligand derivative $\{C_6H_4\text{-}1,2\text{-}[NC(t\text{Bu})N(2,6\text{-}Me_2C_6H_3)]_2\}^{2-}$. Complexes **6** and **7** provide 87 and 92% yield of diethyl hydroxy(phenyl)methylphosphonate, respectively, compared to 44% yield obtained with **2**.

Conclusions

The salt metathesis reactions of $Ln(BH_4)_3(thf)_2$ and $\{C_6H_4\text{-}1,2\text{-}[NC(R)NR']_2\}X_2(thf)_n$ (X = Li, Na; R = *t*Bu, Ph; R′ = 2,6-$Me_2C_6H_3$, $SiMe_3$) in thf in a 1:1 molar ratio afforded a series of lanthanide monoborohydrido complexes $\{C_6H_4\text{-}1,2\text{-}[NC(R)NR']_2\}Ln(BH_4)(L)$ (Ln = Y, Nd, Sm; L = dme, thf) coordinated by bulky *ansa*-bis(amidinato) ligand systems with a conformationally rigid *o*-phenylene linker. Complexes are monomeric and contain a terminal borohydrido ligand. By the example of the yttrium complexes $\{C_6H_4\text{-}1,2\text{-}[NC(Ph)NSiMe_3]_2\}Y(BH_4)(L)_n$ (L = dme, n = 1; L = thf, n = 2), it was demonstrated that the replacement of two molecules of monodentate thf by one bidentate dme in the coordination sphere of yttrium results in the migration of the borohydrido ligand from an equatorial position to an apical one. All complexes are efficient catalysts for the ring-opening polymerization of *rac*-lactide. They allow to convert up to 1000 equiv. of monomer into polymer at room temperature within 10–150 min and to obtain atactic polylactides with high molecular weights and moderate molecular-weight distributions (1.28–2.16). A comparison of the results of the catalytic tests obtained with complexes coordinated by linked bis(amidinato) systems $\{C_6H_4\text{-}1,2\text{-}[NC(t\text{Bu})N(2,6\text{-}Me_2C_6H_3)]_2\}^{2-}$, $\{C_6H_4\text{-}1,2\text{-}[NC(Ph)NSiMe_3]_2\}^{2-}$ and $\{CH_2[CH_2NC(Ph)NSiMe_3]_2\}^{2-}$ clearly demonstrates that both the bulkiness of the substituents at the "external" nitrogen atoms and the rigidity of the linker between the amidinato fragments deeply affect the catalytic activity of the derived complexes and the degree of control of the *rac*-lactide polymerization. The activity of lanthanide–borohydrido complexes in the catalysis of the hydrophosphonylation of aldehydes was demonstrated.

Experimental Section

General: All reactions were performed with rigorous exclusion of air and traces of water by using Schlenk techniques and a vacuum line. All solvents were distilled from sodium/benzophenone and thoroughly degassed. C_6D_6 and C_7D_8 were dried with sodium prior to use and condensed under vacuum into NMR tubes. $CDCl_3$ was used without additional purification. $\{C_6H_4\text{-}1,2\text{-}[NC(t\text{Bu})NH(2,6\text{-}Me_2C_6H_3)]_2\}$,[9a] $\{C_6H_4\text{-}1,2\text{-}[NC(Ph)NSiMe_3]_2\}Li_2(thf)$,[9b] $(Me_3Si)_2NNa$,[21] and $Ln(BH_4)_3(thf)_3$[12] were prepared according to literature procedures. NMR spectra were recorded with Bruker Avance DRX-400 and Bruker DRX-200 spectrometers in C_6D_6, C_7D_8, or $CDCl_3$ at 25 °C, unless otherwise stated. Chemical shifts for ^1H and ^{13}C NMR spectra were referenced internally to the residual solvent resonances and are reported relative to TMS. IR spectra were recorded on Nujol mulls with a Bruker-Vertex 70 spectrophotometer. Lanthanide metal analyses were carried out by complexometric titration.[22] The C, H, N elemental analyses were performed in the microanalytical laboratory of the G. A. Razuvaev Institute of Organometallic Chemistry. GPC was carried out by using a chromatograph "Knauer Smartline" with Phenogel Phenomenex Columns 5u (300 × 7.8 mm) 10^4, 10^5 and a Security Guard Phenogel Column with RI and UV detectors (254 nm). The mobile phase was thf and the flow rate was 2 mL/min. The columns were calibrated by Phenomenex Medium- and High-Molecular-Weight Polystyrene Standard Kits with peak molecular weights from 2700 to 2570000 Da. The number-average molecular masses (M_n) and polydispersity indexes (M_w/M_n) of the polymers were calculated with reference to a universal calibration vs. polystyrene standards. M_n values of PLAs were corrected with a Mark–Houwink factor

of 0.58 to account for the difference in hydrodynamic volumes between polystyrene and polylactide.[23] The microstructures of the PLAs were measured by homo-decoupling ^{1}H NMR spectroscopy at 25 °C in $CDCl_3$ with a Bruker Avance DRX-400 spectroscopy instrument.

Synthesis of {C$_6$H$_4$-1,2-[NC(*t*Bu)N(2,6-Me$_2$C$_6$H$_3$)]$_2$}Y(BH$_4$)(dme) (2): To a solution of **1** (0.44 g, 0.91 mmol) in thf (20 mL) was added a solution of $Na(NSiMe_3)_2$ (0.33 g, 1.80 mmol) in thf (20 mL). The resulting yellow solution was stirred at ambient temperature for 30 min, and the volatiles were removed under vacuum. The solid residue was redissolved in thf (40 mL) and added to a solution of $Y(BH_4)_3(thf)_3$ (0.32 g, 0.91 mmol) in thf (20 mL). The reaction mixture was stirred for 3 days. After removal of thf, the yellow solid was extracted with toluene (60 mL). The extract was filtered, and the solvent was removed under vacuum. The recrystallization of the solid residue from a dme/hexane mixture afforded yellow, transparent crystals (0.32 g, 0.47 mmol). Yield 52%. $C_{36}H_{54}BN_4O_2Y$ (674.56): calcd. C 64.10, H 8.07, N 8.31, Y 13.18; found C 63.97, H 8.12, N 8.25, Y 13.22. ^{1}H NMR (400 MHz, C_6D_6, 25 °C): δ = 1.17 (br. s, 4 H, BH_4), 1.37 [s, 18 H, C(CH_3)$_3$], 2.38 [s, 12 H, C$_6$H$_3$(CH_3)$_3$], 2.83 (s, 6 H, CH_3O, dme), 3.09 (s, 4 H, CH_2O, dme), 6.8 [t, $^3J_{H,H}$ = 7.5 Hz, 3 H, C$_6H_4$, C$_6$H$_3$(CH$_3$)$_2$], 6.92–6.98 [m, 5 H, C$_6H_4$, C$_6$H$_3$(CH$_3$)$_2$], 7.38 (dd, $^3J_{H,H}$ = 6.1 and 3.6 Hz, 2 H, C$_6H_4$) ppm. ^{13}C NMR (100 MHz, C_6D_6, 25 °C): δ = 20.7 [C$_6$H$_3$(*C*H$_3$)$_2$], 29.3 [C(*C*H$_3$)$_3$], 41.3 [$^3J_{Y,C}$ = 2.02 Hz, *C*(CH$_3$)$_3$], 61.6 (*C*H$_3$O, dme), 71.5 (*C*H$_2$O, dme) 119.6, 121.0, 122.1, 123.5, 127.9, 128.2, 130.5, 132.5 141.6, 149.3, [C$_6$H$_4$, *C*$_6$H$_3$(CH$_3$)$_2$], 177.2 ($^2J_{Y,C}$ = 1.6 Hz, N*C*N) ppm. ^{11}B NMR (128 MHz, C_6D_6, 25 °C): δ = –23.6 ppm. IR (KBr): $\tilde{\nu}$ = 2423 (s), 2350 (s), 2233 (s), 1653 (s), 1590 (s), 1568 (s), 1275 (s), 1248 (s), 1097 (s), 1049 (s), 1004 (s), 976 (s), 958 (s), 922 (s), 862 (s), 816 (s), 765 (s), 747 (s), 695 (s), 596 (s) cm^{-1}.

Synthesis of {C$_6$H$_4$-1,2-[NC(*t*Bu)N(2,6-Me$_2$C$_6$H$_3$)]$_2$}Nd(BH$_4$)(dme) (3): An analogous synthetic procedure was used by reacting **1** (0.37 g, 0.76 mmol), $Na(NSiMe_3)_2$ (0.28 g, 1.52 mmol), and $Nd(BH_4)_3(thf)_3$ (0.31 g, 0.76 mmol). Green crystals of **3** were isolated in 43% yield (0.24 g, 0.33 mmol). $C_{36}H_{54}BN_4NdO_2$ (729.89): calcd. C 59.24, H 7.46, N 7.68, Nd 19.76; found C 59.38, H 7.52, N 7.59, Nd 19.80. IR (KBr): $\tilde{\nu}$ = 2451 (s), 2426 (s), 2215 (s), 2152 (s), 1656 (s), 1587 (s), 1581 (s), 1535 (s), 1275 (s), 1245 (s), 1179 (s), 1142 (s), 1094 (s), 1028 (s), 952 (s), 910 (s), 765 (s), 744 (s), 695 (s) cm^{-1}.

Synthesis of [C$_6$H$_4$-1,2-{NC(*t*Bu)N(2,6-Me$_2$C$_6$H$_3$)}$_2$]Sm(BH$_4$)(dme) (4): An analogous synthetic procedure was used by reacting **1** (0.38 g, 0.80 mmol), $Na(NSiMe_3)_2$ (0.29 g, 1.60 mmol), and $Sm(BH_4)_3(thf)_3$ (0.33 g, 0.80 mmol). Yellow crystals of **4** were isolated in 39% yield (0.23 g, 0.31 mmol) yield. $C_{36}H_{54}BN_4O_2Sm$ (736.01): calcd. C 58.75, H 7.40, N 7.61, Sm 20.43; found C 58.53, H 7.46, N 7.55, Sm 20.45. IR (KBr): $\tilde{\nu}$ = 2454 (s), 2215 (s), 2154 (s), 1656 (s), 1581 (s), 1535 (s), 1272 (s), 1245 (s), 1212 (s), 1188 (s), 1170 (s), 1142 (s), 1097 (s), 1031 (s), 956 (s), 910 (s), 765 (s) cm^{-1}.

Synthesis of [C$_6$H$_4$-1,2-{NC(Ph)NSiMe$_3$}$_2$]Y(BH$_4$)(thf)$_2$ (6): To a solution of $Y(BH_4)_3(thf)_3$ (0.22 g, 0.61 mmol) in thf (20 mL) a solution of **5** (0.31 g, 0.286 mmol) in thf (20 mL) was added, and the reaction mixture was stirred for 5 h at 65 °C. The solvent was removed under vacuum, and the remaining solid was extracted with toluene (35 mL), and the extract was filtered. Toluene was evaporated under vacuum, and the remaining solid residue was recrystallized by slow condensation of hexane into a concentrated thf solution. Pale-yellow crystals of **6** were isolated in 67% yield (0.27 g). $C_{34}H_{52}BN_4O_2Si_2Y$ (704.70): calcd. C 57.95, H 7.44, N 7.95, Y 12.62; found C 57.70, H 7.42, N 7.89, Y 12.67. ^{1}H NMR (400 MHz, C_6D_6, 25 °C): δ = 0.20 [s, 5 H, Si(CH_3)$_3$], 0.24 [s, 9 H, Si(CH_3)$_3$], 0.50 [s, 4 H, Si(CH_3)$_3$], 1.35 (br. s, 8 H, β-CH_2, thf), 1.72 (br. s, 4 H, BH_4), 3.65 (br. s, 8 H, α-CH_2, thf), 5.71 (dd, $^3J_{H,H}$ = 7.9 Hz, $^3J_{H,H}$ = 1.4 Hz, 1 H, C$_6H_4$), 6.18–7.31 (m, together 12 H, C$_6H_4$, C$_6H_5$), 7.92 (d, $^3J_{H,H}$ = 7.1 Hz, 1 H, C$_6H_5$) ppm. ^{13}C NMR (100 MHz, C_6D_6, 25 °C): δ = 2.5, 2.9, 3.5 [Si(*C*H$_3$)$_3$], 25.2 (β-*C*H$_2$, thf), 68.2 (α-*C*H$_2$, thf), 116.2, 120.5, 123.0, 125.9, 128.4, 129.7, 130.5, 137.5, 138.4, 140.1, 142.4 (*C*$_6$H$_4$, *C*$_6$H$_5$), 174.7, 185.2 (N*C*N) ppm. ^{11}B NMR (128.4 MHz, C_6D_6, 25 °C): δ = –26.6 ppm. IR (KBr): $\tilde{\nu}$ = 2401 (s), 2338 (s), 2280 (s), 2228 (s), 1608 (s), 1587 (s), 1566 (s), 1489 (s), 1289 (s), 1252 (s), 1236 (s), 1127 (s), 1074 (s), 1023 (s), 964 (s), 914 (s), 845 (s), 802 (s), 791 (s), 757 (s), 735 (s), 703 (s), 674 (s), 629 (s), 568 (s), 530 (s), 464 (s) cm^{-1}.

Synthesis of [C$_6$H$_4$-1,2-{NC(Ph)NSiMe$_3$}$_2$]Y(BH$_4$)(dme) (7): To a solution of $Y(BH_4)_3(thf)_3$ (0.18 g, 0.52 mmol) in thf (20 mL) a solution of **5** (0.28 g, 0.258 mmol) in thf (20 mL) was added, and the reaction mixture was stirred for 5 h at 65 °C. The solvent was removed under vacuum, and the remaining solid was extracted with toluene (35 mL), and the extract was filtered. Toluene was evaporated under vacuum, and the solid residue was dissolved in a dme/toluene mixture (1:1, 20 mL). Cooling the concentrated solution at –20 °C afforded 0.23 g of pale-yellow crystals of **7**. Yield 60%. $C_{37}H_{54}BN_4O_2Si_2Y$ (742.74): calcd. C 59.83, H 7.33, N 7.54, Y 11.97; found C 59.67, H 7.28, N 7.61, Y 12.01. ^{1}H NMR (400 MHz, C_7D_8, 25 °C): δ = 0.04–0.5 [m, together 18 H, Si(CH_3)$_3$], 1.48 (br. s, 4 H, BH_4), 3.18 (br. s, 6 H, CH_3O, dme), 3.28 (br. s, 4 H, CH_2O, dme), 5.60–7.45 (m, together 13 H, C$_6H_4$, C$_6H_5$), 7.90 (d, $^3J_{H,H}$ = 7.0 Hz, 1 H, C$_6H_5$) ppm. ^{13}C NMR (100 MHz, C_7D_8, 25 °C): δ = 2.5, 2.7, 3.4 [Si(*C*H$_3$)$_3$], 58.4 (*C*H$_3$O, dme), 71.7 (*C*H$_2$O, dme), 116.9, 120.6, 122.8, 126.6, 129.6, 129.9, 130.4, 140.0, 140.4, 141.4, 142.3 (*C*$_6$H$_4$, *C*$_6$H$_5$), 174.3, 185.0 (N*C*N) ppm. ^{11}B NMR (128.4 MHz, C_6D_6, 25 °C): δ = –29.1 ppm. IR (KBr): $\tilde{\nu}$ = 2438 (s), 2377 (s), 2251 (s), 1608 (s), 1566 (s), 1510 (s), 1489 (s), 1289 (s), 1241 (s), 1215 (s), 1191 (s), 1124 (s), 1079 (s), 1044 (s), 964 (s), 919 (s), 842 (s), 799 (s), 743 (s), 703 (s), 679 (s), 629 (s), 570 (s), 528 (s), 469 (s) cm^{-1}.

General Procedure for the *rac*-Lactide Polymerization: To a solution of the complex (10 mmol) in toluene (per 1 M solution of lactide) lactide was added. The mixture was immediately stirred with a magnetic stirring bar at 20 °C. The reaction was quenched by adding a solution 10% H_2O in thf (1 mL), and the polymer was precipitated from a CH_2Cl_2/pentane mixture (ca. 2 mL:100 mL) five times. The polymer was dried under vacuum to a constant weight.

General Procedure for the Synthesis of Diethyl Hydroxy(phenyl)-methylphosphonate [C$_6$H$_5$CH(OH)P(O)(OEt)$_2$]: HP(O)(OEt)$_2$ (1 mmol, 0.138 g, 0.127 mL) was added to a solution of benzaldehyde (1 mmol, 0.106 g, 0.101 mL) and catalyst (1×10^{-5} mol) in toluene (2 mL). The reaction mixture was stirred at room temperature for 24 h and was subsequently hydrolyzed with water (1.0 mL), extracted with ethyl acetate (3×10.0 mL), dried with anhydrous Na_2SO_4 and filtered. After the solvent was removed under vacuum, the final product was recrystallized from a thf/hexane mixture. The yield of diethyl hydroxy(phenyl)methylphosphonate was determined by weighing. ^{1}H NMR (400 MHz, $CDCl_3$, 25 °C): δ = 1.18–1.26 (m, 6 H, CH_3CH$_2$O), 3.91–4.08 (m, 4 H, CH$_3$CH_2O), 4.51 (br. s, 1 H, C*H*), 5.00 (d, $^3J_{H,H}$ = 11 Hz, 1 H, O*H*), 7.26–7.48 (m, 5 H, C$_6H_5$) ppm. ^{31}P NMR (162 MHz, $CDCl_3$, 25 °C): δ = 21.5 ppm.

X-ray Crystallography: The X-ray data for **2**–**7** were collected with a Smart Apex diffractometer [graphite-monochromated Mo-K$_\alpha$ radiation, ω-scan technique, λ = 0.71073 Å, T = 100(2) K]. The structures were solved by direct methods and were refined on F^2 by using the SHELXTL[24] package. All non-hydrogen atoms and B-

Table 3. Crystallographic data and structure refinement details for **2**–**7**.

Complex	**2**	**3**	**4**	**6**	**7**
Empirical formula	$C_{36}H_{52}BN_4O_2Y$	$C_{36}H_{54}BN_4NdO_2$	$C_{36}H_{54}BN_4O_2Sm$	$C_{34}H_{52}BN_4O_2Si_2Y$	$C_{37}H_{54}BN_4O_2Si_2Y$
Formula weight	672.54	729.88	735.99	704.70	742.74
T, [K]	100(2)	100(2)	100(2)	100(2)	100(2)
Wavelength [Å]	0.71073				
Crystal system	triclinic	monoclinic	monoclinic	orthorhombic	triclinic
Space group	$P\bar{1}$	$P2(1)$	$P2(1)$	$P2(1)2(1)2(1)$	$P\bar{1}$
a [Å]	12.0009(10)	8.9309(3)	8.9043(5)	11.8602(14)	8.3192(2)
b [Å]	12.6793(10)	15.5558(6)	15.5691(8)	12.3233(15)	14.0383(4)
c [Å]	12.9740(10)	13.2200(5)	13.2033(7)	24.839(3)	18.0087(5)
α [°]	83.473(2)	90	90	90	81.446(1)
β [°]	87.144(2)	100.161(1)	99.968(1)	90	85.643(1)
γ [°]	63.643(1)	90	90	90	73.17
Volume [Å^3]	1757.5(2)	1807.8(1)	1802.8(2)	3630.4(8)	1989.54(9)
Z	2	2	2	4	2
$\rho_{calcd.}$ [g/cm^3]	1.271	1.341	1.356	1.289	1.240
Absorption coefficient, [mm^{-1}]	1.695	1.471	1.664	1.707	1.561
$F(000)$	712	758	762	1488	784
Crystal size [mm]	0.68 × 0.16 × 0.14	0.40 × 0.30 × 0.15	0.40 × 0.30 × 0.15	0.40 × 0.35 × 0.23	0.35 × 0.28 × 0.25
θ range for data collection [°]	1.89 to 27.00	2.04 to 26.00	2.32 to 26.00	2.33 to 25.99	1.82 to 26.00
Index ranges	$-15 \le h \le 15$	$-11 \le h \le 11$	$-10 \le h \le 10$	$-14 \le h \le 14$	$-10 \le h \le 10$
	$-15 \le k \le 16$	$-19 \le k \le 19$	$-19 \le k \le 19$	$-15 \le k \le 15$	$-17 \le k \le 17$
	$-16 \le l \le 16$	$-16 \le l \le 16$	$-16 \le l \le 16$	$-30 \le l \le 30$	$-22 \le l \le 22$
Reflections collected	16097	15675	15615	28842	17160
Independent reflections	7559	7027	7014	6946	7727
R_{int}	0.0280	0.0173	0.0190	0.0464	0.0165
Completeness to θ [%]	98.4	99.5	99.5	98.2	98.7
Absolute structure parameter		–0.017(8)	–0.027(8)	–0.004(5)	
Goodness-of-fit on F^2	1.010	1.087	1.064	1.033	1.046
Final R indices [$I > 2\sigma(I)$]	R_1 = 0.0398	R_1 = 0.0202	R_1 = 0.0206	R_1 = 0.0384	R_1 = 0.0285
	wR_2 = 0.0945	wR_2 = 0.04623	wR_2 = 0.0501	wR_2 = 0.0863	wR_2 = 0.0715
R indices (all data)	R_1 = 0.0547	R_1 = 0.0219	R_1 = 0.0217	R_1 = 0.0475	R_1 = 0.0336
	wR_2 = 0.0992	wR_2 = 0.0470	wR_2 = 0.0507	wR_2 = 0.0891	wR_2 = 0.0732
Largest diff. peak and hole [e/Å^3]	0.960/–0.662	1.368/–0.431	1.406/–0.424	1.034/–0.525	0.517/–0.401

bonded hydrogen atoms were found from Fourier syntheses of electron density. All non-hydrogen atoms were refined anisotropically, whereas B-bonded hydrogen atoms were refined isotropically, and other H atoms were refined isotropically in the riding model. SADABS[25] were used to perform area-detector scaling and absorption corrections. Crystallographic data and collection and refinement details are shown in Table 3, and the corresponding CIF files are available in the Supporting Information. CCDC-940266 (for **2**), -940267 (for **3**), -940268 (for **4**), -940269 (for **6**), and -940270 (for **7**) contain the supplementary crystallographic data for this paper. These data can be obtained free of charge from The Cambridge Crystallographic Data Centre via www.ccdc.cam.ac.uk/data_request/cif.

Supporting Information (see footnote on the first page of this article): The ^{1}H and ^{13}C NMR spectra of complexes **2**, **6**, **7**, and IR spectra of **2**–**4**, **6**, **7** are presented.

Acknowledgments

This work was financially supported by the Russian Foundation for Basic Research (Grants 11-03-00555, 12-03-93109-НЦНИЛ_а, 12-03-31865 mol_a).

[1] R. D. Schannon, *Acta Crystallogr., Sect. A: Found. Crystallogr.* **1976**, *32*, 751–767.

[2] a) F. T. Edelmann, D. M. M. Freckmann, H. Schumann, *Chem. Rev.* **2002**, *102*, 1851–1896; b) W. E. Piers, D. J. H. Emslie, *Coord. Chem. Rev.* **2002**, *233*, 131–155; c) A. A. Trifonov, *Russ. Chem. Rev.* **2007**, *76*, 1051–1072.

[3] For examples of Ln borohydrides see: a) F. Bonnet, A. R. Cowley, P. Mountford, *Inorg. Chem.* **2005**, *44*, 9046–9055; b) I. Palard, A. Soum, S. M. Guillaume, *Chem. Eur. J.* **2004**, *10*, 4054–4062; c) J. Huang, J. F. Yu, G. M. Wu, W. L. Sun, Z. Q. Shen, *Chin. Chem. Lett.* **2009**, *20*, 1357–1360; d) J. Jenter, P. W. Roesky, N. Ajellal, S. M. Guillaume, N. Susperregui, L. Maron, *Chem. Eur. J.* **2010**, *16*, 4629–4638; e) D. Robert, M. Kondracka, J. Okuda, *Dalton Trans.* **2008**, 2667–2669; f) S. M. Guillaume, M. Schappacher, A. Soum, *Macromolecules* **2003**, *36*, 54–60; g) H. E. Dyer, S. Huijser, N. Susperregui, F. Bonnet, A. D. Schwarz, R. Duchateau, L. Maron, P. Mountford, *Organometallics* **2010**, *29*, 3602–3621; h) M. A. Sinenkov, G. K. Fukin, A. V. Cherkasov, N. Ajellal, Th. Roisnel, F. M. Kerton, J.-F. Carpentier, A. A. Trifonov, *New J. Chem.* **2011**, *35*, 204–212; i) T. V. Mahrova, G. K. Fukin, A. V. Cherkasov, A. A. Trifonov, N. Ajellal, J.-F. Carpentier, *Inorg. Chem.* **2009**, *48*, 4258–4266; j) A. A. Trifonov, G. G. Skvortsov, D. M. Lyubov, G. K. Fukin, E. A. Fedorova, M. N. Bochkarev, *Russ. Chem. Bull. Int. Ed.* **2005**, *54*, 2511–2518; k) M. Vissaux, F. Bonnet, *Coord. Chem. Rev.* **2011**, *255*, 374–420.

[4] a) P. Dubois, O. Coulembier, J.-M. Raquez (Eds.), *Handbook of Ring-Opening Polymerization*, Wiley-VCH Verlag GmbH & Co. KGaA: Weinheim, Germany **2009**; b) O. Dechy-Cabaret, B. Martin-Vaca, D. Bourissou, *Chem. Rev.* **2004**, *104*, 6147–6176; c) M. J. Stanford, A. P. Dove, *Chem. Soc. Rev.* **2010**, *39*, 486–494; d) C. M. Thomas, *Chem. Soc. Rev.* **2010**, *39*, 165–173; e) J. Kratsch, M. Kuzdrowska, M. Schmid, N. Kazeminejad, C. Kaub, P. Oña-Burgos, S. M. Guillaume, P. Roesky, *Organometallics* **2013**, *32*, 1230–1238.

[5] a) A.-Ch. Albertson, I. K. Varma, *Biomacromolecules* **2003**, *4*, 1466–1486; b) A. P. Gupta, V. Kumar, *Eur. Polym. J.* **2007**, *43*, 4053–4074; c) R. H. Platel, L. M. Hodgson, C. K. Williams, *Polym. Rev.* **2008**, *48*, 1163.

[6] G. G. Skvortsov, M. V. Yakovenko, P. M. Castro, G. K. Fukin, A. V. Cherkasov, J.-F. Carpentier, A. A. Trifonov, *Eur. J. Inorg. Chem.* **2007**, 3260–3267.

[7] a) F. T. Edelmann, *Coord. Chem. Rev.* **1994**, *137*, 403–481; b) J. Barker, M. Kilner, *Coord. Chem. Rev.* **1994**, *133*, 219–300; c) M. P. Coles, *Dalton Trans.* **2006**, 985–1001; d) F. T. Edelmann, *Adv. Organomet. Chem.* **2008**, *57*, 183–352; e) P. J. Bailey, S. Pace, *Coord. Chem. Rev.* **2001**, *214*, 91–141.

[8] a) M. V. Yakovenko, A. V. Cherkasov, G. K. Fukin, D. Cui, A. A. Trifonov, *Eur. J. Inorg. Chem.* **2010**, 3290–3298; b) M. V. Yakovenko, A. A. Trifonov, E. N. Kirillov, T. Roisnel, J.-F. Carpentier, *Inorg. Chim. Acta* **2012**, *383*, 137–142.

[9] a) A. O. Tolpygin, A. S. Shavyrin, A. V. Cherkasov, G. K. Fukin, A. A. Trifonov, *Organometallics* **2012**, *31*, 5405–5413; b) G. G. Skvortsov, G. K. Fukin, S. Yu. Ketkov, A. V. Cherkasov, K. A. Lyssenko, A. A. Trifonov, *Eur. J. Inorg. Chem.* **2013**, 4173–4183.

[10] W. Li, M. Xue, J. Tu, Y. Zhang, Q. Shen, *Dalton Trans.* **2012**, *41*, 7258–7265.

[11] M. Ephritikhine, *Chem. Rev.* **1997**, *97*, 2193–2242.

[12] a) U. Mirsaidov, I. Shaimuradov, M. Hikmatov, *Zh. Neorg. Khim. (Rus. J. Inorg. Chem.)* **1986**, *31*, 1321–1326; b) B. G. Segal, S. J. Lippord, *Inorg. Chem.* **1978**, *17*, 844–850.

[13] a) M. Visseaux, T. Chenal, P. Roussel, A. Mortreux, *J. Organomet. Chem.* **2006**, *691*, 86–92; b) M. Visseaux, M. Mainil, M. Terrier, A. Mortreux, P. Roussel, T. Mathievet, M. Destarac, *Dalton Trans.* **2008**, 4558–4561; c) P. Zinck, M. Visseaux, A. Mortreux, *Z. Anorg. Allg. Chem.* **2006**, *632*, 1943–1944; d) D. Barbier-Baudry, O. Blacque, A. Hafid, A. Nyassi, H. Sitzmann, M. Visseaux, *Eur. J. Inorg. Chem.* **2000**, 2333–2336; e) S. M. Cendrowski-Guillaume, M. Nierlich, M. Lance, M. Ephritikhine, *Organometallics* **1998**, *17*, 786–788; f) F. Yuan, J. Yang, L. Xiong, *J. Organomet. Chem.* **2006**, *691*, 2534–2539.

[14] a) D. A. Laske, R. Duchateau, J. H. Teuben, A. L. Spek, *J. Organomet. Chem.* **1993**, *462*, 149–153; b) T. J. Marks, G. W. Grynkewich, *Inorg. Chem.* **1976**, *15*, 1302–1307; c) D. Deng, X. Zheng, C. Qian, J. Sun, L. Zhang, *J. Organomet. Chem.* **1994**, *466*, 95–100.

[15] R. D. Schannon, *Acta Crystallogr., Sect. A: Found. Crystallogr.* **1976**, *32*, 751–767.

[16] See for example: A. Amgoune, C. M. Thomas, S. Ilinca, T. Roisnel, J.-F. Carpentier, *Angew. Chem.* **2006**, *118*, 2848; *Angew. Chem. Int. Ed.* **2006**, *45*, 2782–2784 and references cited therein.

[17] a) H. R. Kricheldorf, M. Berl, N. Scharnagi, *Macromolecules* **1988**, *21*, 286–293; b) P. Dubois, C. Jacobs, R. Jérôme, P. Teyssié, *Macromolecules* **1991**, *24*, 2266–2270; c) M. Lahcini, P. M. Castro, M. Kalmi, M. Leskelä, T. Repo, *Organometallics* **2004**, *23*, 4547–4549; d) M. Kalmi, M. Lahcini, P. M. Castro, O. Lehtonen, A. Belfkira, M. Leskelä, T. Repo, *J. Polym. Sci., Part A: Polym. Chem.* **2004**, *42*, 1901–1911.

[18] Y. Nakayama, S. Okuda, H. Yasuda, T. Shiono, *React. Funct. Polym.* **2007**, *67*, 798–806.

[19] A. N. Pudovik, I. V. Konovalova, *Synthesis* **1979**, 81–96.

[20] a) P. Merino, E. Marqués-Lopés, R. P. Herrera, *Adv. Synth. Catal.* **2008**, *350*, 1195–1208; b) S. Zhou, Z. Wu, J. Rong, S. Wang, G. Yang, X. Zhu, L. Zhang, *Chem. Eur. J.* **2012**, *18*, 2653–2659; c) S. Zhou, H. Wang, J. Ping, S. Wang, L. Zhang, X. Zhu, Y. Wei, F. Wang, Z. Feng, X. Gu, S. Yang, H. Miao, *Organometallics* **2012**, *31*, 1696–1702.

[21] L. E. Manzer, *Inorg. Chem.* **1978**, *17*, 1552–1558.

[22] S. J. Lyle, M. M. Rahman, *Talanta* **1953**, *10*, 1177–1182.

[23] I. Barakat, P. Dubois, R. Jerome, P. Teyssié, *J. Polym. Sci. A: Polym. Chem.* **1993**, *31*, 505–514.

[24] G. M. Sheldrick, *SHELXTL v6*.12, Structure Determination Software Suite; Bruker AXS, Madison, WI, **2000**.

[25] G. M. Sheldrick, *SADABS v2.01*, Bruker/Siemens Area Detector Absoption Correction Program; Bruker AXS, Madison, WI, **1998**.

Received: July 21, 2013
Published Online: November 4, 2013

